

Oscillating Hydrodynamical Jets in Steady Shear of Nano-Rod Dispersions

S. Heidenreich, S. Hess, S. H. L. Klapp, M. Gregory Forest, Ruhai Zhou, and Xiaofeng Yang

Citation: **1027**, 168 (2008); doi: 10.1063/1.2964622

View online: <http://dx.doi.org/10.1063/1.2964622>

View Table of Contents: <http://aip.scitation.org/toc/apc/1027/1>

Published by the [American Institute of Physics](#)

Oscillating Hydrodynamical Jets in Steady Shear of Nano-Rod Dispersions

S. Heidenreich ^{a*}, S. Hess ^{*}, S. H. L. Klapp [†], M. Gregory Forest ^{**}, Ruhai Zhou [‡] and Xiaofeng Yang ^{**}

^{*}*Institute for Theoretical Physics, Technische Universität Berlin, D-10623, Germany*

[†]*Stranski-Laboratorium for Physical and Theoretical Chemistry & Institute for Theoretical Physics, Technische Universität Berlin, D-10623, Germany*

^{**}*Department of Mathematics & Institute for Advanced Materials, University of North Carolina at Chapel Hill, Chapel Hill NC27599-3250, US*

[‡]*Department of Mathematics and Statistics, Old Dominion University, Norfolk, VA 23529, US*

Abstract. The dynamical behavior of molecular alignment strongly affects the flow properties of nano-rod dispersions such as nematic polymers. Numerical studies have been performed for the Navier-Stokes equations with an extra stress determined by the rod orientational distribution, coupled to three different orientation models: the Doi-Hess kinetic model, the Doi-Marrucci-Greco tensor model, and the alignment tensor model. We reported spatially localized spurts in the velocity profile, which we call jets, that oscillate, i.e., the jets appear and disappear in periodic fashion [14], generalizing a similar phenomenon reported by Kupferman, Kawaguchi and Denn [2] for a model two-dimensional nematic liquid. The emergence of these oscillatory hydrodynamical jets is due to the competition of elasticity from the rod ensemble and flow coupling; the jet structures coincide with the periodic formation of a disordered phase known as an oblate defect. Here we show a parameter regime where multiple jets arise within the shear gap in the alignment tensor model, reminiscent of multiple shear banding in soft matter systems that possess both locally ordered and disordered phases such as worm-like micelles [3].

Keywords: shear flow, nematic polymers, numerical simulation, structure formation

PACS: 61.30.Vx, 61.30.Hn, 47.50.Cd, 61.30.Jf

INTRODUCTION AND MODELS

The nano-rod dispersion is a general and simple model for a wide range of anisotropic, non-Newtonian fluids that consist of molecules or Brownian particles with properties similar to rigid rods or platelets. Representative examples are liquid crystals, liquid crystal polymers, worm-like micelles, and tobacco mosaic virus suspensions. In each of these model systems, orientational degrees of freedom and the possibility to form different mesoscopic phases (isotropic and nematic) lead to surprising orientational behavior [1, 2] and flow feedback in shear-dominated flows. The large literature on shear banding in sheared worm-like micelles [3] is an example of the remarkable non-Newtonian flow feedback that is possible in such systems.

For the description of the orientational behavior of nano-rod dispersions, three different models are considered. The first model is the kinetic model, where the orientation is described by a generalized Fokker-Planck equation for the rod orientational probability distribution [4] function $f(\mathbf{m}, \mathbf{x}, t)$

$$\frac{D}{Dt}f = \mathcal{R} \cdot [(\mathcal{R}f + f\mathcal{R}V)] - \mathcal{R} \cdot [\mathbf{m} \times \dot{\mathbf{m}}f], \quad \dot{\mathbf{m}} = \Omega \cdot \mathbf{m} + a[\mathbf{D} \cdot \mathbf{m} - \mathbf{D} : \mathbf{m}\mathbf{m}\mathbf{m}], \quad (1)$$

where $D/Dt = \partial/\partial t + \mathbf{v} \cdot \nabla$, $\mathcal{R} = \mathbf{m} \times \frac{\partial}{\partial \mathbf{m}}$ is the rotational gradient operator. \mathbf{D} and Ω are the dimensionless rate-of-strain and vorticity tensors, respectively, and $a = \frac{r^2-1}{r^2+1}$, where r is the rod aspect ratio. The coupled Maier-Saupe and Marrucci-Greco potential is [5] given by $V = -\frac{3N}{2} \mathbf{M} : \mathbf{m}\mathbf{m} - \frac{1}{2Er} [\Delta \mathbf{M} + \theta \nabla \nabla \cdot \mathbf{M}] : \mathbf{m}\mathbf{m}$, with the rank-2 tensor $\mathbf{M} = \mathbf{M}(f) = \int_{|\mathbf{m}|=1} \mathbf{m}\mathbf{m} f(\mathbf{m}, \mathbf{x}, t) d\mathbf{m}$. Here N is a dimensionless rod volume fraction which governs the strength of short-range excluded volume interactions. The Ericksen number (Er) measures short-range nematic potential strength relative to distortional elasticity strength. For other parameters we refer to [6]. The other models considered here are of Landau-de Gennes type, where the probability distribution function $f(\mathbf{m}, \mathbf{x}, t)$ of the kinetic theory is projected onto the second moment tensor, \mathbf{M} . The orientation tensor \mathbf{Q} is the trace zero form of \mathbf{M} , $\mathbf{Q} = \mathbf{M} - \frac{1}{3}$. The distinctions among

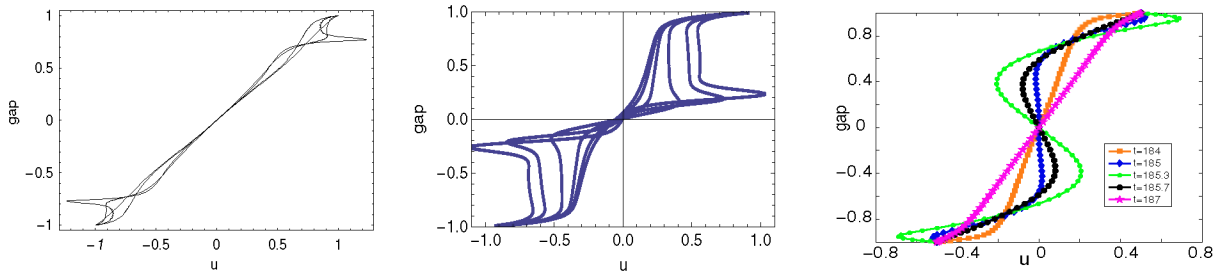


FIGURE 1. Snapshots of the primary velocity profile across the shear gap from the kinetic model (left), the alignment tensor model (middle) and the Doi-Marrucci-Greco model (right).

models can be framed in terms of closure rules that are necessary to reduce the above coupled flow-kinetic orientation model to relaxation equations. The relaxation equation of the Doi-Marrucci-Greco model is given by [5, 7]:

$$\begin{aligned} \frac{D}{Dt} \mathbf{Q} &= \Omega \mathbf{Q} - \mathbf{Q} \Omega + a(\mathbf{D} \mathbf{Q} + \mathbf{Q} \mathbf{D}) + \frac{2a}{3} \mathbf{D} - 2a \mathbf{D} : \mathbf{Q} \left(\mathbf{Q} + \frac{\mathbf{I}}{3} \right) \\ &- \left(\mathbf{F}(\mathbf{Q}) + \frac{1}{3Er} (\Delta \mathbf{Q} : \mathbf{Q} \left(\mathbf{Q} + \frac{\mathbf{I}}{3} \right) - \frac{1}{2} (\Delta \mathbf{Q} \mathbf{Q} + \mathbf{Q} \Delta \mathbf{Q}) - \frac{1}{3} \Delta \mathbf{Q} \right), \mathbf{F}(\mathbf{Q}) = \left(1 - \frac{N}{3} \right) \mathbf{Q} - N \mathbf{Q}^2 + N \mathbf{Q} : \mathbf{Q} \left(\mathbf{Q} + \frac{\mathbf{I}}{3} \right). \end{aligned} \quad (2)$$

The third model was originally derived within the framework of irreversible thermodynamics. In principle the relaxation equation can be obtained by projection of the kinetic model to the second moment tensor with appropriate closure rules [8]:

$$\begin{aligned} \frac{D}{Dt} \mathbf{Q} &= \Omega \mathbf{Q} - \mathbf{Q} \Omega + \kappa \left(\mathbf{D} \mathbf{Q} + \mathbf{Q} \mathbf{D} - \frac{2}{3} (\mathbf{D} : \mathbf{Q}) \mathbf{I} \right) + \bar{D}_a \left(\Delta \tilde{\mathbf{F}}(\mathbf{Q}) - \frac{\tilde{D}e}{\tilde{E}r} \Delta^2 \mathbf{Q} \right) - \frac{1}{\tilde{D}e} \tilde{\mathbf{F}}(\mathbf{Q}) + \frac{1}{\tilde{E}r} \Delta \mathbf{Q} - \sqrt{\frac{3}{2}} \lambda_K \mathbf{D}, \\ \tilde{\mathbf{F}}(\mathbf{Q}) &= \vartheta \mathbf{Q} - 3\sqrt{6} (\mathbf{Q} \mathbf{Q} - \frac{1}{3} (\mathbf{Q} : \mathbf{Q}) \mathbf{I}) + 2 \frac{(\mathbf{Q} : \mathbf{Q}) \mathbf{Q}}{1 - \frac{(\mathbf{Q} : \mathbf{Q})^2}{Q_{max}^4}}. \end{aligned} \quad (3)$$

Note, that all three models contain elasticity terms and flow orientational couplings. In our analysis we consider plane Couette flow, such that a one-dimensional physical space heterogeneity (in the gap between the two parallel plates) can be assumed. The no-slip boundary conditions on the velocity $\mathbf{v} = (u(y), 0, 0)$ imply $u(y = \pm 1, t) = \pm De$. We assume homogeneous tangential anchoring at the plates, given by the quiescent nematic equilibrium, $f(\mathbf{m}, y = \pm 1, t) = f_e(\mathbf{m})$, where $f_e(\mathbf{m})$ is an equilibrium solution of the Smoluchowski equation corresponding to the tangential anchoring of particles at the plates when $\mathbf{v} = \mathbf{0}$, or equivalently in the Landau type models, $\mathbf{Q}_{eq} = s(\mathbf{e}_x \mathbf{e}_x - \frac{1}{3} \mathbf{I})$, where $\mathbf{e}_x = (1, 0, 0)$. The velocity profile is determined through momentum balance equation $d\mathbf{v}/dt = \nabla \cdot (-p\mathbf{I} + \boldsymbol{\tau})$ where the stress tensor $\boldsymbol{\tau}$ is slightly different for each model (see [6, 7, 8]).

RESULTS AND DISCUSSION

The partial differential equations for all three models were solved numerically and local pulsating spurts of the velocity were observed [14]. In Fig. 1 from [14], snapshots are shown of the primary flow profile during, before, and after the jet pulses form for the three models. The exact shape and the location of the jet is different as expected when different models and different parameter values are compared. However, in every model local pulsating spurts exist. The hydrodynamic feedback phenomenon shown above arises from orientational gradients in the stress constitutive law, whose divergence couples to the Navier-Stokes momentum balance. This anisotropic non-Newtonian flow behavior is then correlated with orientation, and found to be associated with disordered defect phases. One space-dimensional behavior cannot be associated with topological defects; instead, for each model we found an orientational oblate defect phase that coincides with each jet ‘‘pulse’’. The space-time correlations between oblate defect phases [9] and jet layers are amplified through the ellipsoid graphics (see Fig2a, from [14]). In each model, we find so-called wagging orbits (a finite amplitude oscillation in the principal axis of orientation) which continuously grow in amplitude from the plates to the jet-defect layer, and then the major director tumbles more or less in phase in the interior of the

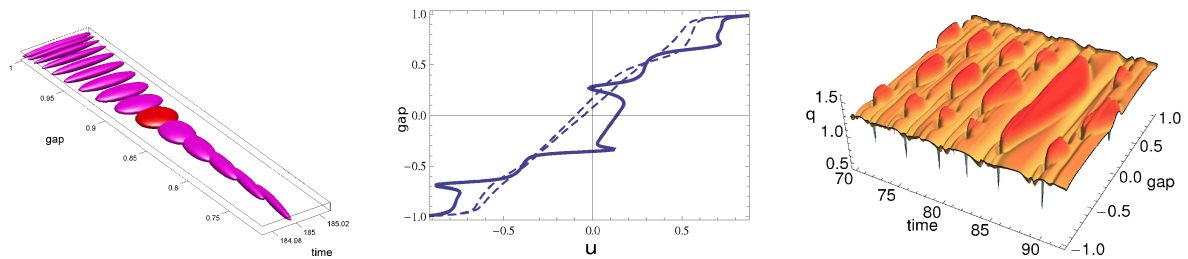


FIGURE 2. (a) The second-moment tensor ellipsoids of the Doi-Marrucci-Greco model simulation from [14]. (b) Snapshots of the primary velocity profile across the gap in the alignment tensor model in a different parameter regime than reported in [14]. (c) Space time surface plot of the order parameter q for alignment tensor model for the same parameters as in Figure 2b.

shear gap. In [14], we reported parameter regimes with a single pulsating jet-defect layer in each half of the shear gap. Here we extend these simulations, Figure 2b,c, to find a more complex pulsating shear band structure, with four jets across the gap. Thus we find alternating layers of wagging and tumbling, with jets and oblate defect phases forming at the layer transitions. These phenomena are reminiscent of defect gas-like textures in [11] (without flow feedback).

We note that the formation of composite tumbling-wagging 1D heterogeneous attractors have been observed previously, including studies of Tsuji and Rey [10] and the authors [9], where in-plane symmetry was imposed and pure shear was also imposed. The present simulations do not enforce in-plane symmetry, and solve for the fully coupled flow, yet we find the space-time attractor is in-plane; the out-of-plane degrees of freedom in the tensor and full kinetic distribution function simply decay to zero. The conditions on De and Er simply have to be tuned to amplify the flow feedback jet phenomenon where the flow profile becomes non-monotonic and jet-like layers arise.

A major achievement of all three models lies in their prediction of sign changes in the first normal stress difference, N_1 , typically associated with the tumbling transition in classical experiments of Kiss and Porter [12]. Here, we have heterogeneous and dynamical resolution in the flow and orientational distribution; we find (see [14]) layers of negative N_1 coincide in space and time with jet-oblate defect layers!

ACKNOWLEDGEMENTS This research was supported in part by the National Science Foundation grant DMS 0604891, NASA-URETI BImat Award NCC-1-02037 and AFOSR contract FA9550-06-1-0063 and the Sonderforschungsbereich 448.

REFERENCES

1. G. Rienäcker, M. Kröger, and S. Hess, Phys. Rev. E **66** 040702(R) (2002); M. Grosso, R. Keunings, S. Crescitelli, and P.L. Maffettone, Phys. Rev. Lett. **86**, 3184 (2001); M.G. Forest, Q. Wang and R. Zhou, Rheol. Acta, **80** (2004).
2. H. Zhou, M.G. Forest, Q. Wang, Discrete and Continuous Dyn. Syst. B, **707** (2007); B. Chakrabarti, M. Das, C. Dasgupta, S. Ramaswamy, A.K. Sood, Phys. Rev. Lett. **92**, 055501, (2004); M.G. Forest, R. Zhou, Q. Wang, Modeling of Soft Matter, IMA **141**, 85-98, (2005); R. Kupferman, M. Kawaguchi, M. M. Denn, J. Non-Newtonian Fluid Mechanics, **91**, 255 (2001); D.H. Klein, L.G. Leal, C. Cervera, and H. Ceniceros, Phys. of Fluids, **19**, 023101 (2007).
3. S.M. Fielding and P.D. Olmsted, Phys. Rev. Lett. **90**, 224501, (2003); R. Lopez-Gonzalez, W.M. Holmes, P.T. Callaghan and P.J. Photinos, Phys. Rev. Lett. **93**, 268302 (2004).
4. S. Hess, Z. Naturforsch **31a**, 1034 (1976); M. Doi, J. Polym. Sci., Polym. Phys. **19**, 229 (1981)
5. G. Marrucci, F. Greco, Mol. Cryst. Liq. Cryst. **206**, 17-30 (1991); G. Marrucci, F. Greco, Adv. Chem. Phys. **86**, 331-404 (1993).
6. Q. Wang, J. Chem. Phys., **116** (20), 9120-9136 (2002).
7. H. Zhou, M.G. Forest, Q. Wang, Disc. Contin. Dyn. Syst. Ser. B, **8** (3), 707-733 (2007).
8. S. Heidenreich, P. Ilg, and S. Hess, Phys. Rev. E. **73**, 061710 (2006); C. Pereira Borgmeyer, S. Hess, J. Non-Equilib. Thermodyn. **20**, 359-384 (1995); S. Hess, Z. Naturforsch. **30a**, 728, 1224 (1975).
9. M.G. Forest, R. Zhou, Q. Wang, Multiscale Model. Simul. **4**(4), 1280-1304 (2005).
10. T. Tsuji, A.D. Rey, Phys. Rev. E **62**, 8141-8151 (2000).
11. D. Grecov and A.D. Rey, Phys. Rev. E **68**, 061704 (2003)
12. G. Kiss, R.S. Porter, *J. Polymer Sci., Polym. Phys. Ed.* **18**, 361 (1980).
13. X. Yang, Z. Cui, M.G. Forest, Q. Wang, J. Shen, Multiscale Model. Simul. (2008) in press.
14. appears in the J. Non-Newton. Fluid Mech.